AIMS Materials Science, 9(6): 835–862.
DOI: 10.3934/matersci.2022051
Received: 28 May 2022
Revised: 16 September 2022
Accepted: 29 September 2022
Published: 25 October 2022

http://www.aimspress.com/journal/Materials

Research article

Investigating the effect of cryogenic treatment of workpieces and tools on electrical discharge machining performance

Vijaykumar S Jatti[1,*], Nitin K Khedkar[2], Vinaykumar S Jatti[2] and Pawandeep Dhall[3]

[1] Symbiosis Institute of Technology, Symbiosis International (Deemed University), Pune, India
[2] Symbiosis Institute of Technology, Symbiosis International (Deemed University), Pune, India
[3] Department of Mechanical Engineering (Robotics), University of California Berkeley, CA, USA

* **Correspondence:** Email: vijaykumar.jatti@sitpune.edu.in.

Abstract: In this competitive world, manufacturers must embrace new technology in order to differentiate their products and capture market leadership. This can be achieved using advanced materials; however, these materials are difficult to machine by using traditional machining processes. A very viable and practical unconventional machining process is electrical discharge machining (EDM). EDM processes need proper selection of input parameters to get optimum productivity aspects, namely, the material removal rate and tool wear rate. Thus, the present study aims at investigating the effect of cryogenically treated work pieces and tools, gap currents, gap voltages, pulse on time and pulse off time on the material removal rate and tool wear rate during EDM of Nitinol (NiTi) alloy, Monel (NiCu) alloy and beryllium copper (BeCu) alloy. The experimental results showed that cryogenic treatment significantly improved the electrical conductivity of the workpieces and tool electrodes, which resulted in an enhanced material removal rate and reduced tool wear rate.

Keywords: beryllium copper alloy; Monel alloy; shape memory alloy; cryogenic treatment; electrical conductivity

1. Introduction

Typical conventional machining processes cannot cope with the properties of new materials, such as stiffness, high strength and hardness. Among the most widely used machining methods for such advanced materials is electrical discharge machining (EDM). Optimum performance can be attained

by optimizing different process parameters for machining different materials. An important aspect of die sinking EDM is the proper selection of the manufacturing conditions, as these conditions determine significant features, such as the surface roughness (SR), material removal rate (MRR) and tool wear rate (TWR). The performance characteristics have been improved by several researchers. This operation is complex by nature and involves many variables; however, the full potential of this process cannot be fully realized. The following paragraphs describes the research undertaken by researches on different combinations of workpiece and tool materials, along with the EDM conditions.

Sharma et al. [1] reduced the number of experiments and extracted the most information from the study using the Box-Bhenken design of the response surface methodology. The electrical properties of electrodes treated with long soaking durations were enhanced by cryogenic treatments, which results in improved wear resistance. Moreover, the results obtained from the experimental results are validated by using a numerical thermodynamic model. To increase productivity of the cryogenically treated EDM process, the proposed model can be used in place of experimental methods. Tharian et al. [2] worked with a non-conventional machining operation in EDM, which allows machining of materials regardless of their hardness or strength. In addition to its advantages, EDM has a low MRR. The effect of cryogenically treated graphite electrodes on the MRR was studied during the machining of Inconel 718. Cryo-treated graphite electrodes improved the MRR in the experiments. Singh et al. [3] did an evaluation between Cu electrodes, rapid manufactured electrodes without cryogenic cooling and electrodes cooled with cryogenic cooling to compare the TWR and SR. With and without cryogenic cooling, the electrodes and machined workpieces were studied for surface characteristics. The cryogenic cooling had a significant effect on the SR and TWR. The rapid dissipation of heat from the surface of the electrode after machining resulted in smoother surfaces, fewer cracks and less debris on the surface of the workpiece machined with the rapidly machined electrode with cryogenic cooling. A comparison of rapidly manufactured electrodes with and without cryogenic cooling showed fewer cracks and less carbon deposition as a result of machining. This is compared with rapidly manufactured electrodes without cryogenic cooling. In electrodes produced using cryogenic cooling, the sharp corner edges of the complex shape tool were preserved after machining because of the low melting point and low vaporization rate of the electrode material. As compared to rapidly manufactured electrodes without cryogenic cooling, rapidly manufactured electrodes with cryogenic cooling were able to produce complex shape features on the workpiece with greater accuracy.

Prakash et al. [4], using micro-EDM, compared the cryogenically treated tool electrode made from the magnesium alloy AZ31B with untreated electrodes. By cryogenically treating the tools, the mechanical properties of the electrodes were enhanced. This included the hardness and wear resistance, which ultimately improved the quality of the machined features. The cryogenically treated tool electrode significantly improved machining performance. Shastri et al. [5] reviewed the limitations of EDM and the approaches adopted by the researchers to overcome these limitations. Various approaches includes cryogenic cooling, powder-mixed EDM, cryogenic treatment, ultrasonic-assisted EDM and other methods. The authors depicted the improvement in EDM performance measures with regard to approaches and notified the future directions in EDM. Abdulkareem et al. [6] used copper electrodes and analyzed the effect of cryogenic cooling while applying EDM to the titanium alloy Ti–6Al–4V. Liquid nitrogen at a temperature of −195 ℃ was used as a coolant. By applying liquid nitrogen to titanium alloys, electrode wear was reduced by 27% and SR by 8%. Gill and Singh [7] investigated the effects of deep cryogenic treatment on the machinability of the titanium alloy Ti-6246

when it was subjected to electrical discharge drilling. Improvements in the MRR and TWR were as high as 8.5% and 34.78%, respectively. Improvements in SR at the base of holes was 9.01%, at the sidewalls of holes was 6.69% and at the overcutting region was 16.09%. It was concluded that electrical discharge drilling with Ti-6246 alloy was significantly improved by deep cryogenic treatment.

Srivastava and Pandey [8] examined the shape of electrodes during the EDM of high-speed steel of M2 grade. As a result of using copper electrodes, and for dielectric medium kerosene oil, was used; after reviewing the results, the researchers concluded that the out-of-roundness of cryogenically cooled electrodes is smaller than that of conventional EDM electrodes. An increased discharge current led to greater out-of-roundness. With the increase in pulse on time, the out-of-roundness was also reduced. Compared to the electrodes used in the experiment without liquid nitrogen, there was little distortion in electrode shape. Yildiz et al. [9] examined the machinability of beryllium copper alloys with −150 ºF and −300 ºF cooling treatments. The tool electrode was copper, and the dielectric medium was EDM-244 oil. The results of the experiments showed that cold and cryogenic treatment processes increased material removal by about 20–30%. For future EDM machinability research, they suggested that a variety of electrode–workpiece material pairs that are subjected to cold and cryogenic processes be used. Singh and Singh [10] conducted an experimental study of the impact of cryogenic treatment on titanium machining characteristics during EDM. This study aimed to examine how the tool and workpiece behaved before and after cryogenic treatment. In their study, they found that there was a 60.39%, 58.77%, 7.99% and 80.00% improvement in MRR, TWR and SR, respectively, with cryogenic treatment.

Gill and Kumar [11] researched the effectiveness of cryogenic treatments in reducing tool wear during EDM. To test whether deep cryogenic treatment reduces tool wear, they used hot die steel (AISI H11) and aluminium tool materials. Nadig et al. [12] worked with a cryo-treatment, and the material was tempered, which improved the thermal conductivity by a small margin. In addition, they highlighted opportunities for future research, suggesting that the cryo-treatment and temperature-related parameters such as time and temperature can be further optimized. Srivastava and Pandey [13] studied the effects of machining high-speed steel M2 using an ultrasonic-assisted cryogenically cooled copper electrode (UACEDM). Using normal electrodes, cryogenically cooled electrodes and ultrasonic-assisted cryogenically cooled electrodes, their MRR, TWR and SR values were compared with those of their EDM counterparts. Compared to conventional EDM, the UACEDM process resulted in lower EWR and SR values, while the MRR was comparable to conventional EDM in terms of the process parameters. The workpieces machined using UACEDM had a higher surface integrity than those machined using conventional EDM. Furthermore, they noted that UACEDM allowed for better retained shapes than conventional EDM. Liqing and Yingjie [14] improved the speed and surface quality, and they applied dry and cryogenically cooled oxygen-mixed EDM. At the chosen experimental conditions, oxygen-mixed dry EDM improved the MRR by more than 200% compared with non-oxygen EDM. An oxygen-mixed air system with a high MRR has been found in a two-gas mixture. Electronegativity and the lower electron affinity energy of oxygen were the other two main factors contributing to an increased MRR during oxygen-mixed dry EDM. The MRR and SR also improved with dry EDM by using cryogenically cooled workpieces under the chosen experimental conditions. Compared with uncooled pieces, the MRR and SR improved approximately 30–50% and 1–10%, respectively.

Jafferson and Hariharan [15] compared the micro-EDM performance of cryo-treated and

untreated microelectrodes, along with the electrical resistivity, crystallite size and microscopic analysis. The study found that the TWR was reduced by 58% for tungsten electrodes, 51% for brass electrodes and 35% for copper electrodes. The electrodes made of tungsten exhibited remarkable improvement in electrical conductivity and micro-hardness, while those made of brass and copper experienced the same improvement. The MRR for all three cryogenically treated electrodes decreased almost proportionately with a decrease in the TWR. Mathai et al. [16] examined the effect of cryogenic treatment on the MRR, TWR and SR. An increased wear rate of tool electrodes was observed when cryogenic treatment was applied. The SR and MRR have been observed to be less influenced by it. Ram et al. [17] determined the effect of the EDM parameters on cryogenically treated and non-cryogenically treated workpieces (EN31); two comparisons were undertaken. To test Taguchi's orthogonal array and establish empirical relations between the MRR, TWR and SR, the researchers used Taguchi's orthogonal array. The cryogenic treatment improved the MRR in these studies; however, the improvement in SR did not reach the same level. Kumar and Kumar [18] described how copper electrodes in EDM were cryogenically cooled using liquid nitrogen. Grey relational analysis was used to optimize the electrode environment, discharge current, pulse on time and gap voltage during the machining of AlSiC metal matrix composites. The experiments were performed using Taguchi's orthogonal array, and the significant parameters were determined via ANOVA. Scanning electron microscopy was used to study the characteristics of the machined surface.

Based on the literature survey, it has been observed that the cryogenic conditions for steel, copper, nickel and their alloys have been studied by few researchers. Cryogenic processes can be used for different electrode–workpiece pairs, which is at a nascent stage based on the available literature. In EDM, a comprehensive comparison of the machining performance of cryogenically treated workpieces and electrodes, along with their electrical parameters, is less reported. Thus, the present work aims at facilitating an understanding of the effect of cryogenically treated workpiece–electrode materials, gap current, pulse off time and pulse on time on the MRR and TWR.

2. Materials and methods

Figure 1a shows an electrical discharge machine. Cryo-treated and untreated copper tool electrodes were used to drill mesoscale square holes of 3 mm × 3 mm with a 5-mm depth onto cryo-treated and untreated workpiece surfaces. In Figure 1b, the top surface of the workpiece was adjusted to be parallel to the tooltip surface using a dial gauge in order to make the electrode setup. The workpiece materials selected were Monel (NiCu) alloy, NiTi alloy and BeCu alloy. Known for their unique properties, these advanced materials have become promising candidates for all types of industries. Literature on the EDM of these alloys is sparse in terms of research papers and books. In addition to NiCu and NiTi alloys of 20 mm × 20 mm × 20 mm, BeCu alloy of 20 × 20 × 30 mm^3 was used. Because electrolytic copper has a high electrical conductivity, it was chosen for experimentation. From the market, we purchased a copper rod measuring 6 mm in diameter and 2000 mm in length. After that, it was cut to 6 mm in diameter and 90 mm in length. Using a milling machine, these pieces were then machined into 3 mm × 3 mm × 25 mm pieces. Figure 1c depicts the workpiece and tool electrode used in the present study. Listed in Table 1 are the chemical, physical and thermoelectric properties of the materials used for the workpieces and tools.

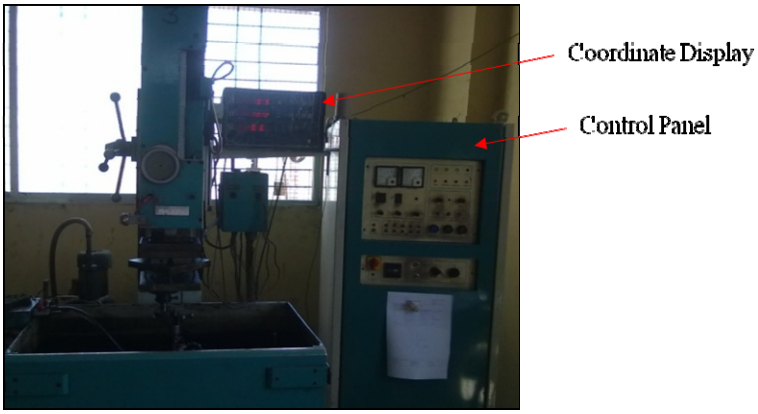

(a) Die sink EDM machine.

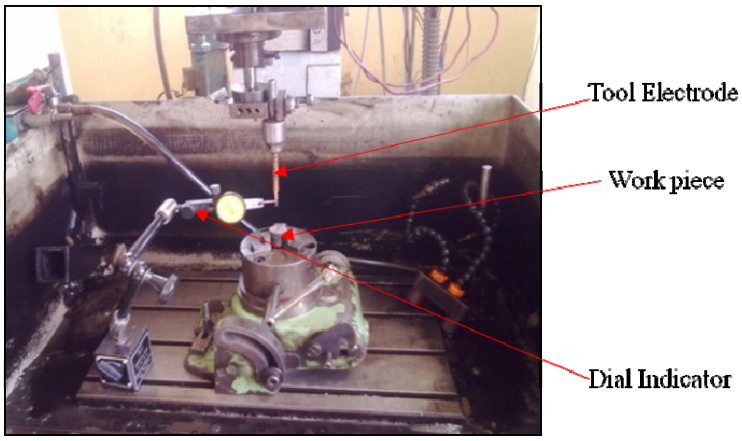

(b) Work piece-tool set up.

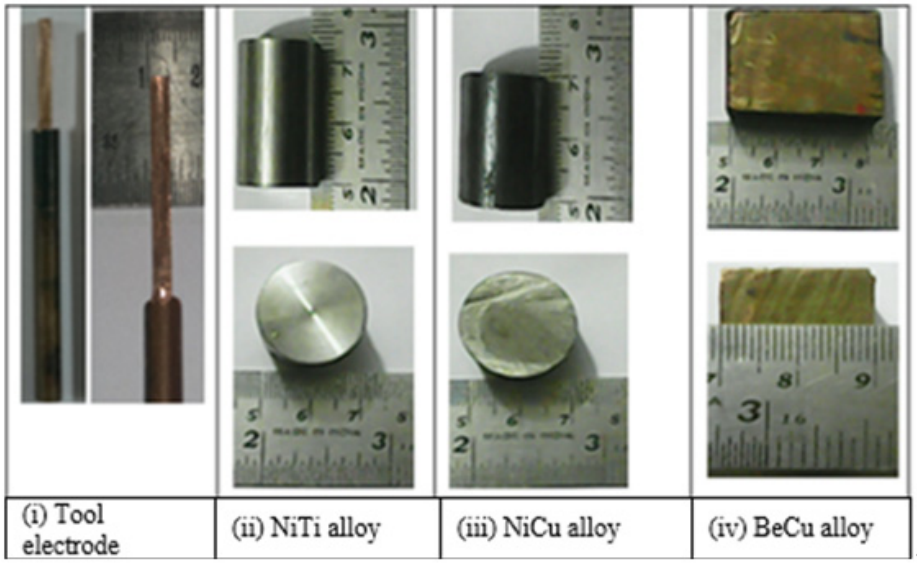

(c) Photographs of work piece and tool materials.

Figure 1. Experimental setup.

Table 1. Material properties.

Properties	NiTi alloy		NiCu alloy		BeCu alloy		Copper electrode	
	Untreated	Treated	Untreated	Treated	Untreated	Treated	Untreated	Treated
Chemical composition	60% Ni, 40% Ti		72% Ni, 28% Cu		2% Be, 98% Cu		99.9% Cu	
Density (ρ), g/cc	6.45		8.8		8.25		8.94	
Specific heat capacity (c_p), J/gK	0.320		0.427		0.420		0.394	
Melting point (H_m), K	1583		1623		1253		1356	
Thermal conductivity (k), W/mK	10	12.9	21.8	22.2	130	135.9	391.1	
Electrical conductivity (σ), S/mm	3.268	4.219	5.515	5.625	5.645	5.902	10	26.316

Cryogenically treating the workpiece and tool before conducting the experiments was a significant step in the process, as shown in Figure 2a,b. There are three main phases to cryogenic treatment. During the first phase of cooling, the temperature gradually decreases from room temperature to −185 ℃. In the second step, the solution is soaked at −185 ℃ for 24 h. The third stage involves tempering the material, which reduces brittleness and improves ductility. Tempering involves heating the material to 150 ℃ in just 2 h, after which it is soaked for 4 h at that temperature. As shown in Figure 2b, the temperature was lowered to room temperature after soaking.

The cryogenic process parameters include the minimum temperature, soaking time, cooling rate and warming rate. In the literature, researchers used different values of these parameters during the cryogenic treatment of different materials. Following are the guidelines based on the literature and industry experts for the selection of the values of these process parameters:

(1) In some cases, the actual T_{min} could be higher than the nominal one because of thermal insulation limits, especially after significant exploitation of the system and the consequential aging of the chamber seals.
(2) Each new material needs to be treated and tested at different temperature levels in order to identify the optimum conditions. In most cases, two or three temperature levels (i.e., −185 °C, −130 ℃ and −80 ℃) are enough to obtain a quick indication in the selection of a specific temperature by means of microstructural changes investigation.
(3) A soaking time of over 36 h does not bring significant improvements and, in most cases, 24 h is enough to obtain results.
(4) The cooling rate value range is restricted in order to prevent thermal-shock cracking. Commonly, the applied values vary from 0.25 ℃/min to 0.5 ℃/min.
(5) In many cryogenic systems, the warming rate is not precisely controllable and little importance to this parameter is given in literature, despite there being some suggested hypotheses about carbide precipitation during the warming phase. The material is brought back to room temperature at a rate of approximately 2.5 ℃/min.

Tempering is the process of reheating the material at predetermined temperatures, which must be lower than the transformational temperature, to obtain required material properties. Tempering reduces residual stresses, increases ductility and toughness and ensures dimensional stability.

To determine the effects of cryogenic treatment on workpiece and tool electrodes, we performed an electrical conductivity test. The illustration in Figure 3 shows the test circuit. A multimeter was used

to measure the current and voltage in the system. The system also included a DC regulator and a holding fixture in addition to the resistors.

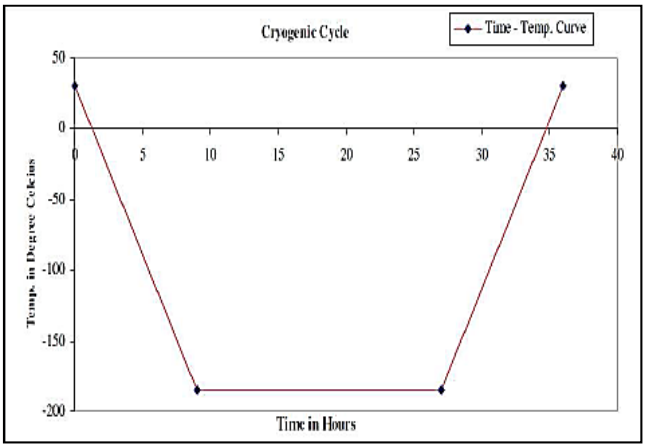

(a) Cycle of cryogenic treatment

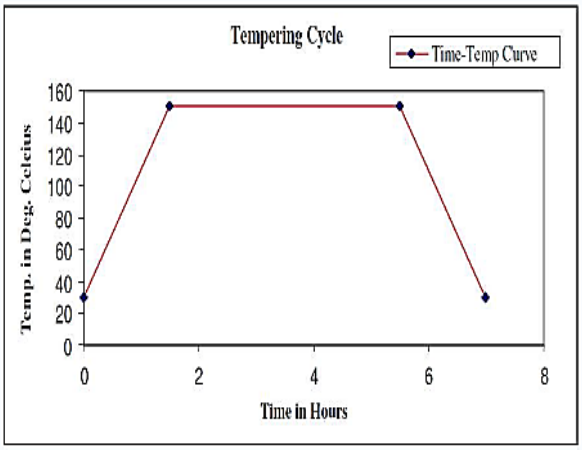

(b) Tempering cycle

Figure 2. Cryogenic treatment process.

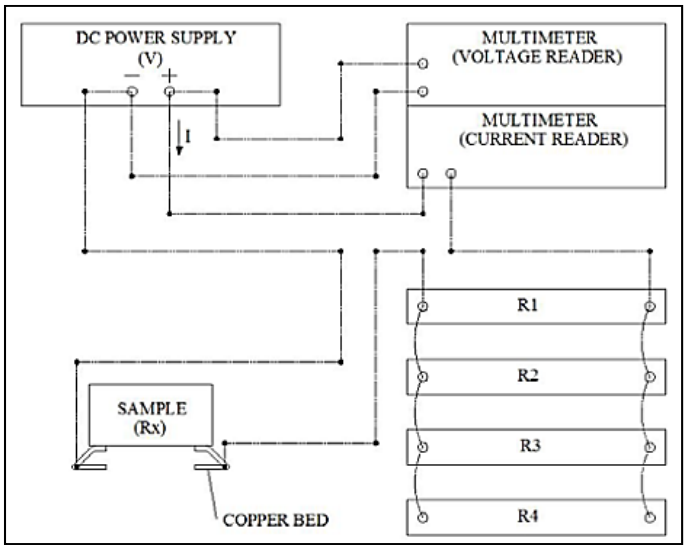

Figure 3. Test rig for measuring electrical conductivity.

Two measures of performance were used in the present study, namely, the MRR and TWR. Weighing was done before and after the machining of the workpiece and tool. This was done by utilizing a digital weighing balance (model: GR-300) with an accuracy of 0.0001 g. The MRR and TWR were calculated by using Eqs 1 and 2.

$$MRR = \frac{\Delta W}{\rho_w \times t_m} \tag{1}$$

ΔW is the change in the weight of the workpiece in grams; ρ_w is the workpiece density, gm/cm^3; t_m is

the machining time in minutes.

$$TWR = \frac{\Delta T}{\rho_t \times t_m} \tag{2}$$

ΔT is the change in the weight of the tool in grams; ρ_T is the tool electrode density, gm/cm^3.

For this study, the EDM process variables were the gap voltage, gap current and the pulse on-off times. Sensitivity for the anti-arc and servo motors was set at 50% and 25%, respectively. Depending on the favorable machining conditions, the workpiece and the tool were used as the negative and positive electrodes, respectively. Therefore, we considered reverse polarity in all experiments. Besides the electrical parameters, the treatment of the workpieces/tools was also analyzed as a parameter. The formulation of the operational ranges for the process parameters was a result of a literature review, favorable machining conditions and sparks.

For each experiment, the machining time was kept constant, but a depth of 5 mm was achieved on the workpiece; instead of keeping the machining time constant, one factor at a time was employed in the first experiment. This method studies the MRR and TWR by using a single process variable and a mean value for other processes. The experiments were performed for each process parameter; five levels were considered. Although this approach cannot clarify the phenomenon pertaining to performance measures, it can provide insight into their essential aspect in relation to the process parameters. In this approach, the range of the process parameters can be identified and the main experiments can be narrowed down based on these parameters. As shown in Table 2, the process variables and other process parameters were set to the most favorable values. We used electrolytic oxygen-free copper (Cu) to machine three kinds of metals, including NiTi, Monel alloy (NiCu) and BeCu. All three materials were drilled with square holes. Other combinations included combinations of untreated workpieces and Cu and cryo-treated workpieces and cryo-treated Cu.

Table 2. Process parameters for exploratory experiments.

Parameters	Values	Performance measures
Gap current (A)	8, 10, 12, 14, 16	MRR and TWR
Gap voltage (V)	40, 48, 55, 63, 70	
Pulse on time (μs)	13, 26, 38, 51, 63	
Pulse off time (μs)	5, 6, 7, 8, 9	
Workpiece/tool cryogenic treatment	Untreated and treated	
Dielectric	Commercial EDM oil	
Flushing pressure (kg/cm^2)	0.5	
Polarity	W.P (-ve); T.E (+ve)	
Tool electrode shape and size	Square 3 × 3 × 25 mm^3	

3. Result and discussions

The results are discussed for four different combinations of workpiece and tool treatments, focusing on the MRR and TWR, including the gap voltage, gap current, pulse on-off duration and the effects of gap current and voltage.

3.1. Effect of gap current on performance measures

In steps of 2 A, the gap current was varied from 8 A to 16 A. Regardless of the treatment of the workpiece or tool, the MRR increased with increasing gap current, as depicted in Figure 4. The cryo-treated Cu and NiTi alloys showed the highest MRR of the four workpiece and tool treatment combinations. The MRR was 1.935 mm^3/min with a gap current of 8 A, and it increased to 4.908 mm^3/min with a gap current of 16 A. In addition, we have found that the treated NiTi alloys and treated Cu have lower TWR values. An 8 A gap current produced a TWR value of 0.0015 mm^3/min, while a gap current of 16 A produced a value of 0.0456 mm^3/min. The TWR increased with increasing gap current, regardless of the workpiece or tool treatment, as shown in Table 3 and Figure 5.

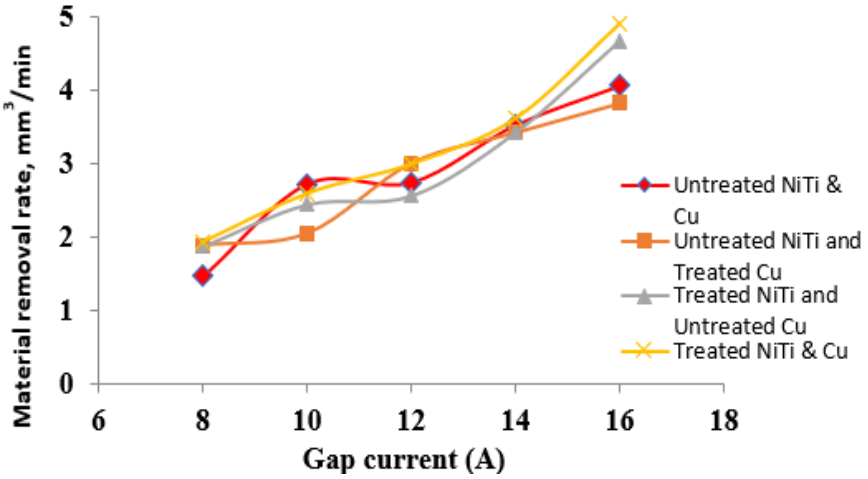

Figure 4. MRR versus gap current for NiTi alloy.

Table 3. Results of exploratory experiments for NiTi alloy (gap current).

Sr. No.	Gap Current (A)	Untreated NiTi and Cu		Untreated NiTi and treated Cu		Treated NiTi and untreated Cu		Treated NiTi and treated Cu	
		MRR (mm^3/min)	TWR (mm^3/min)	MRR (mm^3/min)	TWR (mm^3/min)	MRR (mm^3/min)	TWR (mm^3/min)	MRR (mm^3/min)	TWR (mm^3/min)
1	8	1.465	0.0028	1.884	0.0086	1.872	0.0017	1.935	0.0015
2	10	2.721	0.0091	2.049	0.0110	2.440	0.0089	2.591	0.0080
3	12	2.741	0.0119	3.005	0.0240	2.560	0.0205	2.992	0.0124
4	14	3.523	0.0373	3.419	0.0423	3.424	0.0384	3.615	0.0292
5	16	4.056	0.0758	3.818	0.0543	4.671	0.0979	4.908	0.0456

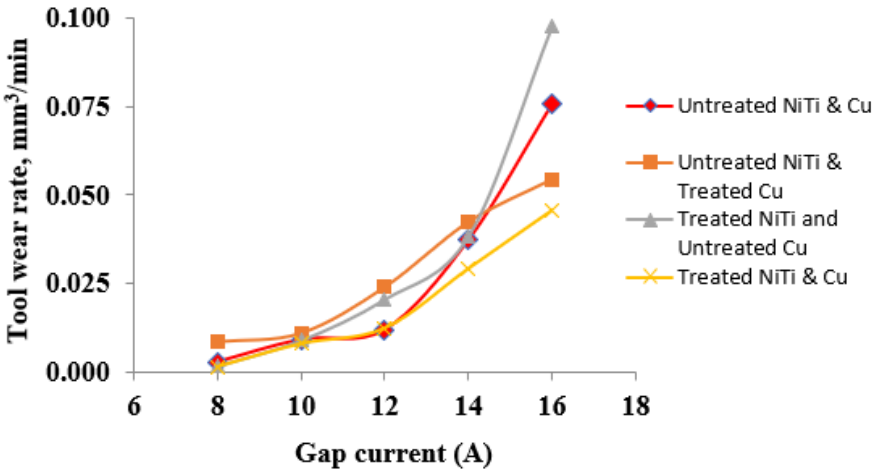

Figure 5. TWR versus gap current for NiTi alloy.

The results of experimentally measuring the gap current and the corresponding performance of the NiCu alloy are shown in Figures 6 and 7. An MRR plot of the NiCu alloy for four-part treatment combinations is shown in Figure 6. Table 4 and Figure 6 show that the MRR and deviation current increased as the deviation current increased. Treatments of the NiCu alloys and Cu resulted in higher MRR values. Figure 7 shows that the TWR varied with the NiCu alloy tools based on the deviation current. The MRR went from 5.401 mm^3/min with a range current of 8 A to 6.849 mm^3/min with a cut-off current of 8 A at 16 A. Figure 8 and Table 4 indicate that the TWR increased with an increasing air gap current. Combining NiCu with treated Cu resulted in a lower TWR value. A cut-off current of 8 A resulted in a TWR of 0.0238 mm^3/min, and a cut-off current of 16 A resulted in a TWR of 0.0673 mm^3/min.

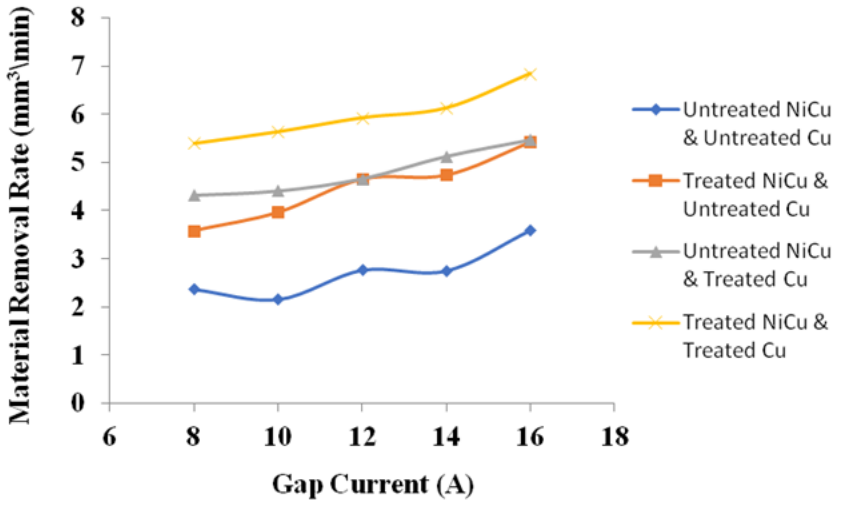

Figure 6. MRR versus gap current for NiCu alloy.

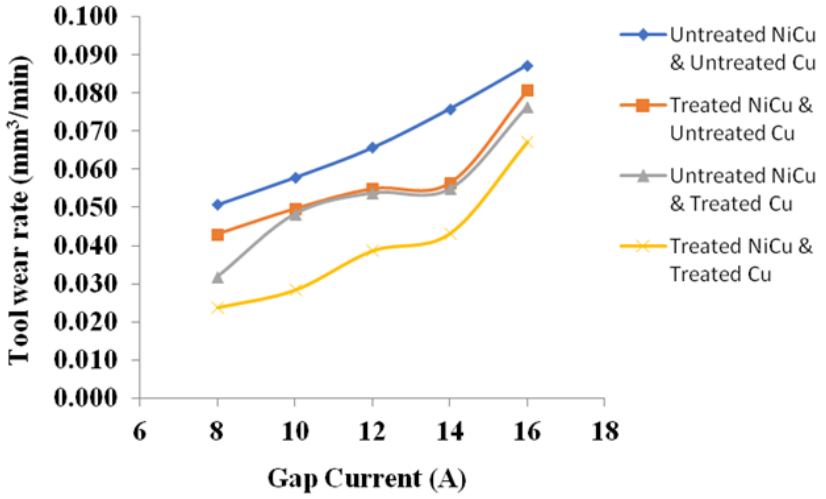

Figure 7. TWR versus gap current for NiCu alloy.

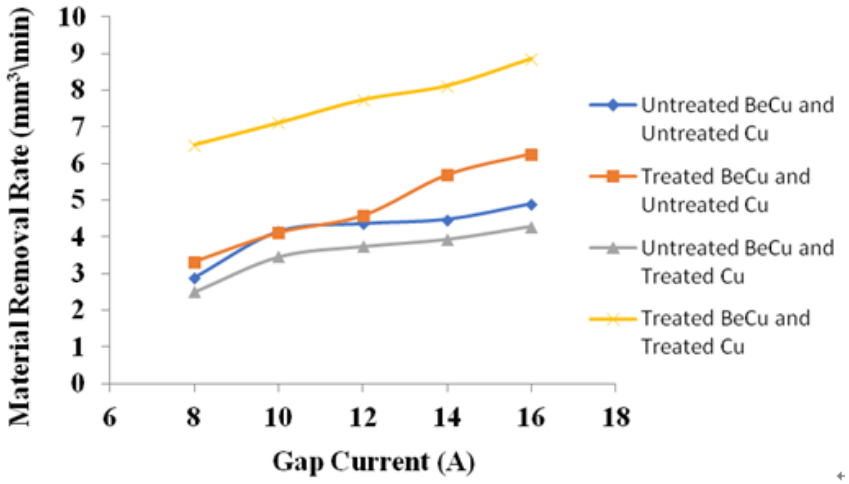

Figure 8. MRR versus gap current for BeCu alloy.

Table 4. Results of exploratory experiments for NiCu alloy (gap current).

Sr. No.	Gap current (A)	Untreated NiCu and Cu		Untreated NiCu and treated Cu		Treated NiCu and untreated Cu		Treated NiCu and treated Cu	
		MRR (mm^3/min)	TWR (mm^3/min)	MRR (mm^3/min)	TWR (mm^3/min)	MRR (mm^3/min)	TWR (mm^3/min)	MRR (mm^3/min)	TWR (mm^3/min)
1	8	2.372	0.0508	4.327	0.0319	3.584	0.0430	5.401	0.0238
2	10	2.167	0.0579	4.416	0.0483	3.966	0.0496	5.645	0.0285
3	12	2.773	0.0657	4.668	0.0538	4.658	0.0549	5.933	0.0387
4	14	2.758	0.0759	5.130	0.0549	4.739	0.0564	6.138	0.0433
5	16	3.596	0.0874	5.469	0.0765	5.422	0.0807	6.849	0.0673

Various gap currents were used to vary the BeCu alloy's performance, and the results are shown in Table 5.

Table 5. Results of exploratory experiments for BeCu alloy (gap current).

Sr. No.	Gap current (A)	Untreated BeCu and Cu		Untreated BeCu and treated Cu		Treated BeCu and untreated Cu		Treated BeCu and treated Cu	
		MRR (mm^3/min	TWR (mm^3/min	MRR (mm^3/min)	TWR (mm^3/min)	MRR (mm^3/min)	TWR (mm^3/min)	MRR (mm^3/min	TWR (mm^3/min)
1	8	2.884	0.0554	2.504	0.0458	3.315	0.0634	6.506	0.0372
2	10	4.136	0.0704	3.454	0.0619	4.105	0.0723	7.103	0.0418
3	12	4.351	0.0848	3.734	0.0770	4.571	0.0887	7.735	0.0497
4	14	4.467	0.0973	3.929	0.0848	5.684	0.1088	8.116	0.0521
5	16	4.894	0.1299	4.281	0.1124	6.256	0.1678	8.856	0.0629

The figure shows three combinations of workpiece–tool treatments for the BeCu alloy in terms of the MRR versus the gap current. The MRR increased as the gap current increased, as can be seen in Table 5 and Figure 8. A higher percentage of material was removed from the treated BeCu and treated Cu as compared to the other combinations. Based on these parameters, the MRR varied from 6.506 mm^3/min with an 8-A gap current to 8.856 mm^3/min with a 16-A gap current. Figure 9 depicts how the TWR varied with the gap current based on the workpiece tools. Treatment of the BeCu and Cu reduced the TWRs. Tool wear was measured at a gap current of 8 A and a gap current of 16 A. At an 8-A gap current, it was 0.0372 mm^3/min, and at a 16-A gap current, it was 0.0629 mm^3/min.

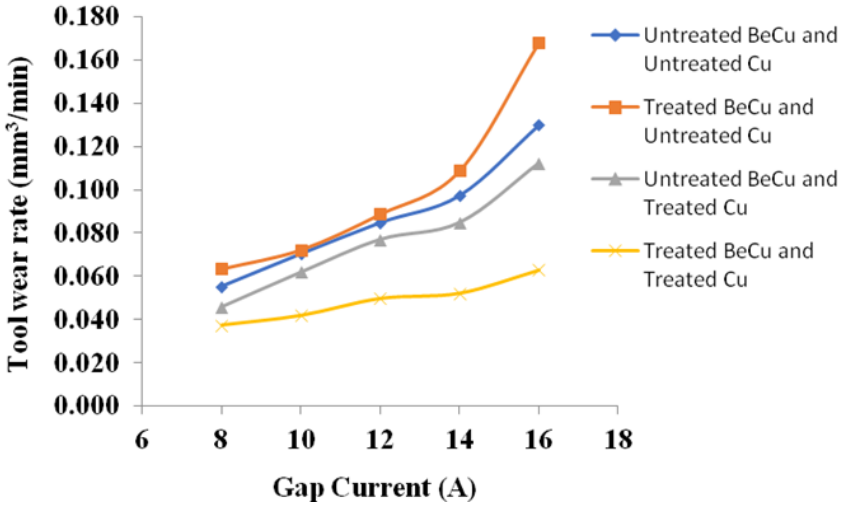

Figure 9. TWR versus gap current for BeCu alloy.

The cryogenic treatment increased the MRR by 123.036% and decreased the TWR by 42.188% for the NiCu material and copper electrode. The MRR and TWR increased by 12.014% and 23.219%, respectively, for the NiTi alloy. The cryogenic treatment of the BeCu alloy and copper electrodes resulted in an increase in the MRR and a decrease in the TWR of 87.548% and 42.587%, respectively.

3.2. Effect of gap voltage on performance measures

There were five levels of gap voltage, keeping other parameters constant. This includes the gap current, pulse on time and pulse off time. Tables 6–8 provide experimentally measured performance data for the NiTi, NiCu and BeCu alloys. As a result of varying the gap voltage for the NiTi alloy, the following results were obtained. According to Figure 10, the MRR rates increased from 40 V to 55 V. At a gap voltage of 55 V, the maximum MRR (8.450 mm^3/min) was achieved for the treated NiTi alloy and treated Cu combination.

Table 6. Results of exploratory experiments for NiTi alloy (gap voltage).

Sr. No	Gap voltage (V)	Untreated NiTi and Cu		Untreated NiTi and treated Cu		Treated NiTi and untreated Cu		Treated NiTi and treated Cu	
		MRR (mm^3/min)	TWR (mm^3/min)	MRR (mm^3/min)	TWR (mm^3/min)	MRR (mm^3/min)	TWR (mm^3/min)	MRR (mm^3/min)	TWR (mm^3/min)
1	40	4.833	0.0966	5.443	0.0757	5.128	0.0883	5.357	0.0586
2	48	5.427	0.0635	6.218	0.0522	5.742	0.0782	6.603	0.0494
3	55	7.123	0.0575	7.248	0.0458	6.664	0.0642	8.450	0.0412
4	63	6.185	0.0446	6.835	0.0390	6.613	0.0594	7.262	0.0378
5	70	5.730	0.0355	6.168	0.0343	6.159	0.0487	6.440	0.0315

Table 7. Results of exploratory experiments for NiCu alloy (gap voltage).

Sr. No.	Gap voltage (V)	Untreated NiCu and Cu		Untreated NiCu and treated Cu		Treated NiCu and untreated Cu		Treated NiCu and treated Cu	
		MRR (mm^3/min)	TWR (mm^3/min)	MRR (mm^3/min)	TWR (mm^3/min)	MRR (mm^3/min)	TWR (mm^3/min)	MRR (mm^3/min)	TWR (mm^3/min)
1	40	2.700	0.0924	3.068	0.0671	3.721	0.0711	3.484	0.0542
2	48	3.560	0.0788	3.889	0.0580	4.402	0.0603	4.951	0.0422
3	55	5.072	0.0637	5.476	0.0529	5.719	0.0586	6.686	0.0350
4	63	4.468	0.0596	5.027	0.0473	5.198	0.0493	5.916	0.0284
5	70	3.201	0.0473	4.360	0.0349	4.538	0.0443	4.808	0.0259

Table 8. Results of exploratory experiments for BeCu alloy (gap voltage).

Sr. No.	Gap voltage (V)	Untreated BeCu and Cu		Untreated BeCu and treated Cu		Treated BeCu and untreated Cu		Treated BeCu and treated Cu	
		MRR (mm^3/min)	TWR (mm^3/min)	MRR (mm^3/min)	TWR (mm^3/min)	MRR (mm^3/min)	TWR (mm^3/min)	MRR (mm^3/min)	TWR (mm^3/min)
1	40	3.683	0.3047	3.431	0.2442	3.592	0.2820	3.999	0.1904
2	48	4.935	0.2584	5.020	0.1831	5.091	0.2041	5.702	0.1401
3	55	5.288	0.1997	6.301	0.1398	6.505	0.1939	7.368	0.1171
4	63	4.382	0.1782	5.478	0.1125	5.549	0.1622	6.040	0.0916
5	70	2.957	0.1615	4.755	0.0976	4.438	0.1476	5.011	0.0838

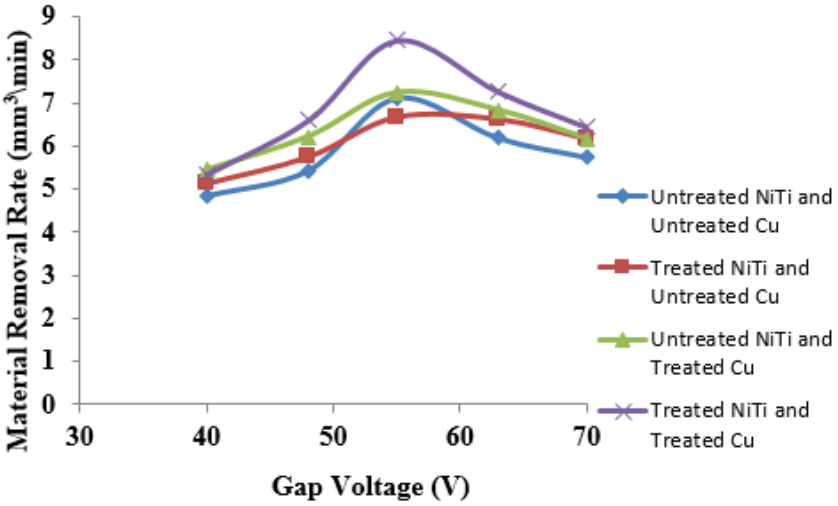

Figure 10. MRR versus gap voltage for NiTi alloy.

The relationship between the TWR and gap voltage is shown in Figure 11 for the NiTi alloy. The TWR decreased as the gap voltage increased. Low gap voltages demonstrate this trend. All four combinations of workpieces and tools show the lowest TWR with the treated Cu and NiTi alloy.

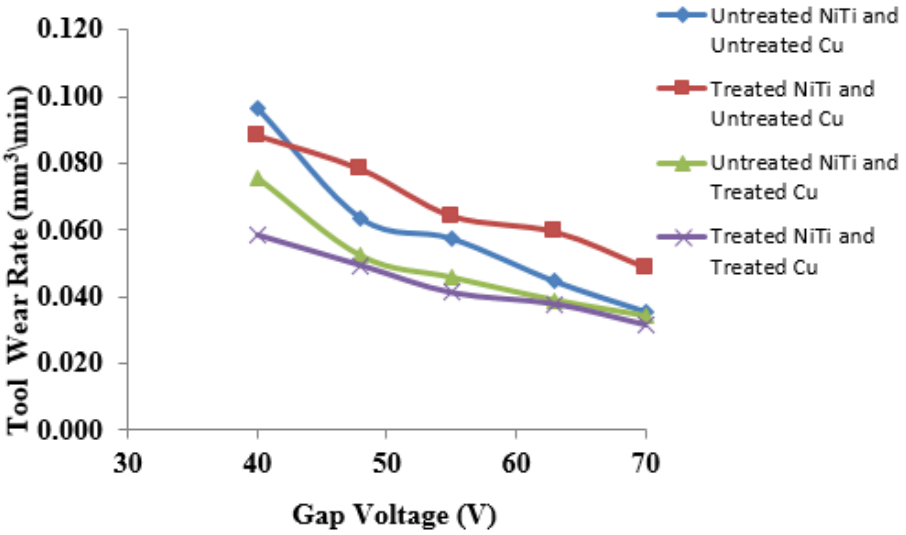

Figure 11. MRR versus gap voltage for NiTi alloy.

Table 7 illustrates the results of applying the tool–workpiece treatment with various gap voltages for different combinations of the NiCu alloy. Figure 12 shows the MRR for NiCu alloys as a function of the gap voltage. A rise from 40 to 55 V occurred for each combination, and a decline from 55 to 70 V followed. Treating NiCu with Cu yielded the highest MRR of the four combinations. A gap voltage of 55 V yielded the maximum MRR for the NiCu alloy and Cu when the gap voltage was 55 V. Figure 13 illustrates how the gap voltage affected the TWR for a variety of combinations of Cu and NiCu alloy. At lower gap voltages, the TWR increased; then, the TWR decreased with

increases in gap voltage. Treatment of the NiCu alloy and treatment of the Cu resulted in lower TWRs than all other combinations.

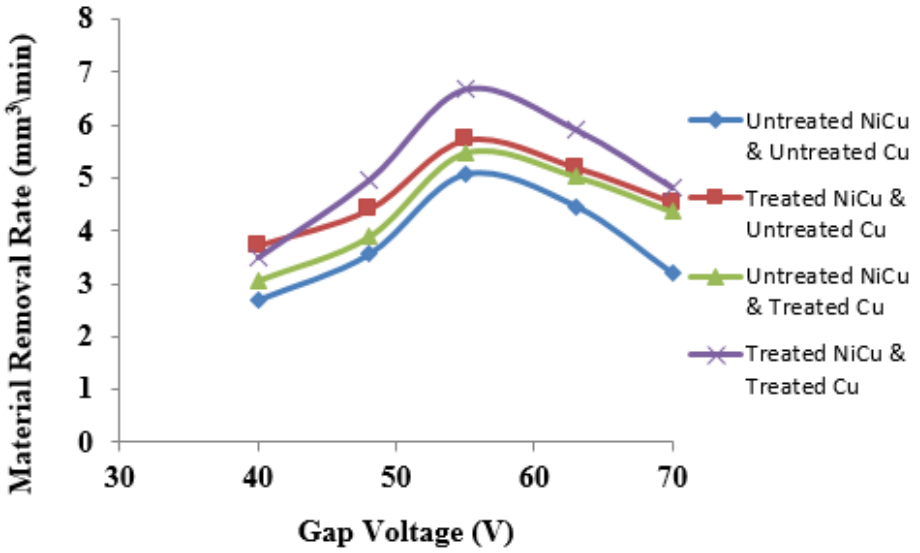

Figure 12. MRR versus gap voltage for NiCu alloy.

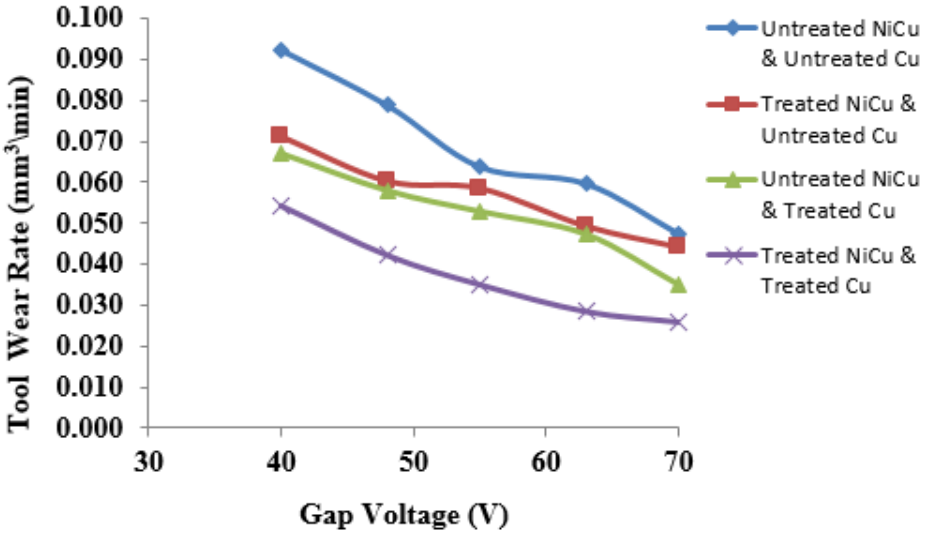

Figure 13. TWR versus gap voltage for NiCu alloy.

The experimental results presented in Table 8 for the BeCu alloy are based on different combinations of tool and workpiece treatment. In Figure 15, for the four combinations of Cu and BeCu, we show how the MRR changed with the gap voltage. Using the figure, the MRR for all combinations reached a maximum at 55 V. The highest MRR was achieved for the treated BeCu-Cu. The maximum MRR (7.368 mm^3/min) was obtained when the gap voltage was 55 V.

The effect of varying the gap voltage on different compositions of Cu and BeCu alloy is shown in Figure 14. Low gap voltages resulted in higher TWRs, and high gap voltages resulted in lower

TWRs, as can be seen from Figure 15. Compared to the other two alloys and corresponding copper combinations, the treated BeCu alloy and treated Cu had lower TWRs.

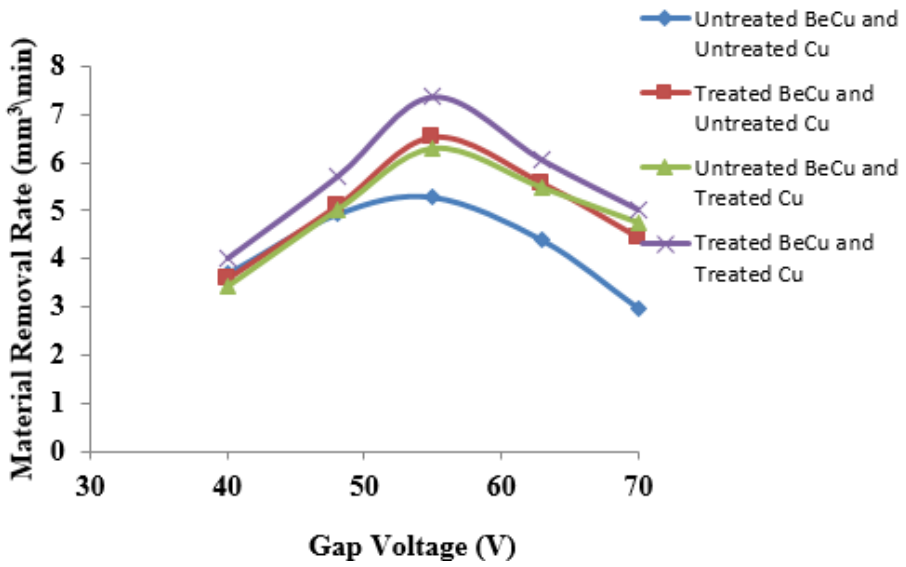

Figure 14. MRR versus gap voltage for BeCu alloy.

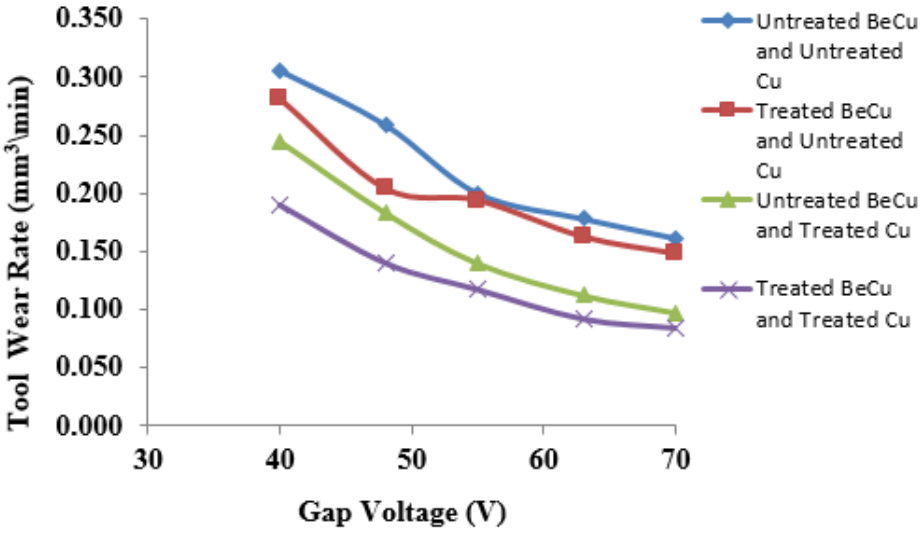

Figure 15. MRR versus gap voltage for BeCu alloy.

The MRR of the cryo-treated Cu electrode and NiTi alloy increased by 16.190%, and the TWR decreased by 23.244%; the MRR of the cryo-treated NiCu alloy and copper electrode increased by 36.504%, and the TWR decreased by 46.103%; and, the MRR of the cryo-treated Cu electrode and BeCu increased by 34.155%, and the TWR decreased by 44.272%.

3.3. Impact of pulse on time on performance measures

Using an interval of 5 seconds, the gap capacitor parameter was varied. The remaining input

parameters were the gap current, gap voltage and pulse off time, i.e., 12 A, 55 V and 7 µs, respectively. Table 9 depicts the exploratory experiments results for NiTi alloy and Cu combinations in regards with pulse on time. The MRR versus pulse on time plot is shown in Figure 16 for four different workpieces and tools. Each workpiece–tool combination had a maximum MRR of 3.924 mm^3/min at a 26-µs pulse on time. Both the NiTi alloy and Cu material had a maximum MRR of 3.924 mm^3/min at a 26-µs pulse on time.

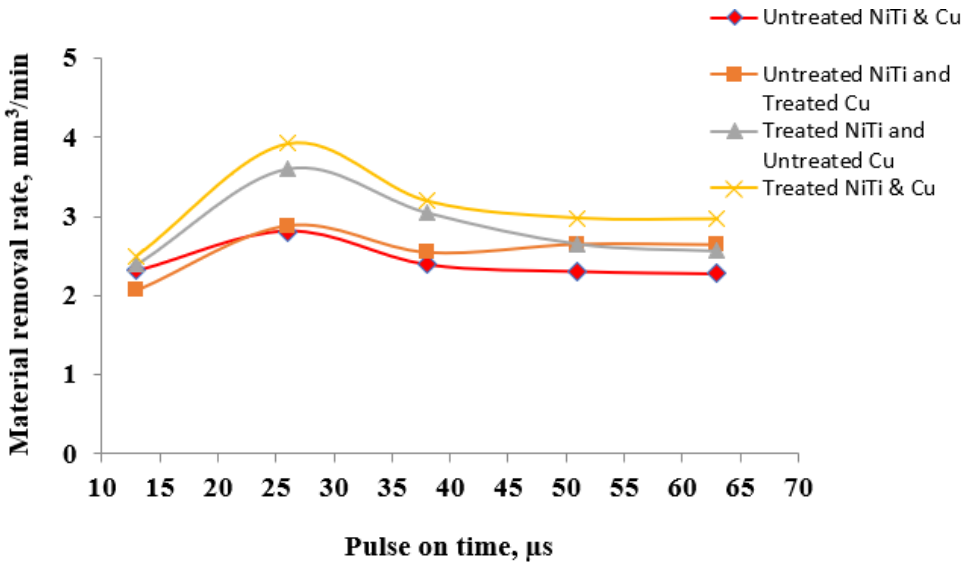

Figure 16. MRR versus pulse on time for NiTi alloy.

Table 9. Results of exploratory experiments for NiTi alloy (pulse on time).

Sr. No.	Pulse on time (µs)	Untreated NiTi and Cu		Untreated NiTi and treated Cu		Treated NiTi and untreated Cu		Treated NiTi and treated Cu	
		MRR (mm^3/min)	TWR (mm^3/min)	MRR (mm^3/min)	TWR (mm^3/min)	MRR (mm^3/min)	TWR (mm^3/min)	MRR (mm^3/min)	TWR (mm^3/min)
1	13	2.315	0.0208	2.066	0.0267	2.393	0.0287	2.499	0.0244
2	26	2.807	0.0621	2.876	0.0586	3.602	0.0724	3.924	0.0484
3	38	2.391	0.0237	2.542	0.0233	3.049	0.0285	3.196	0.0278
4	51	2.305	0.0190	2.645	0.0224	2.654	0.0255	2.980	0.0243
5	63	2.277	0.0166	2.639	0.0211	2.566	0.0234	2.969	0.0224

For the NiTi alloy and Cu combinations, Figure 17 shows the relationship between pulse on time and TWR; TWR increased with increasing pulse on time, until 26 µs, at which point it began decreasing. The same pattern can be observed for all four NiTi alloy and Cu combinations. The treated NiTi and Cu alloys delivered the lowest TWRs among the four combinations.

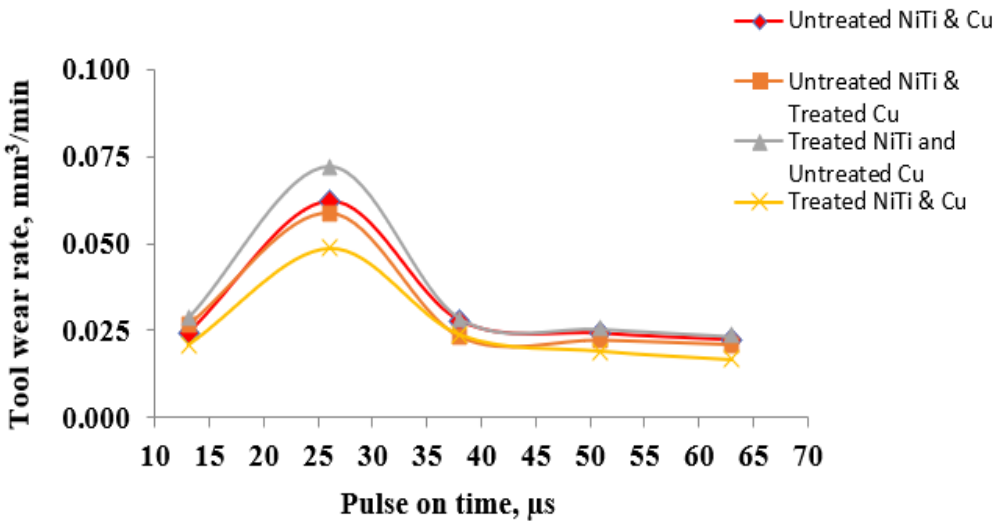

Figure 17. TWR versus pulse on time for NiTi alloy.

As shown in Table 10, experiments with different Cu and NiCu alloys yielded different results. The MRR increased up to a 26-µs pulse on time, but it decreased as the pulse on time increased for the NiCu alloy and Cu combinations. For the cryo-treated Cu and NiCu alloy, the maximum MRR values occurred beyond the pulse on time of 26 µs. The maximum MRR (8.507 mm^3/min) for this combination was obtained when the pulse on time was 26 µs, as can be seen in Figure 18. A comparison of the TWR for the NiCu alloy and Cu combinations is shown in Figure 19. The TWR initially increased and reached 26 µs with increasing pulse on time. After that, the TWR decreased with a greater pulse on time. The treated NiCu alloys and treated copper alloys had the lowest TWR.

Table 10. Results of exploratory experiments for NiCu alloy (pulse on time).

Sr. No.	Pulse on time (µs)	Untreated NiCu and Cu		Untreated NiCu and treated Cu		Treated NiCu and untreated Cu		Treated NiCu and treated Cu	
		MRR (mm^3/min)	TWR (mm^3/min)	MRR (mm^3/min)	TWR (mm^3/min)	MRR (mm^3/min)	TWR (mm^3/min)	MRR (mm^3/min)	TWR (mm^3/min)
1	13	3.424	0.1541	3.676	0.1306	3.877	0.1238	4.457	0.1026
2	26	6.250	0.1818	6.549	0.1607	7.309	0.1666	8.507	0.1220
3	38	4.279	0.0987	5.183	0.0865	5.488	0.0919	7.067	0.0709
4	51	3.951	0.0891	4.359	0.0735	4.949	0.0733	5.532	0.0620
5	63	3.696	0.0788	4.135	0.0688	4.448	0.0631	4.547	0.0478

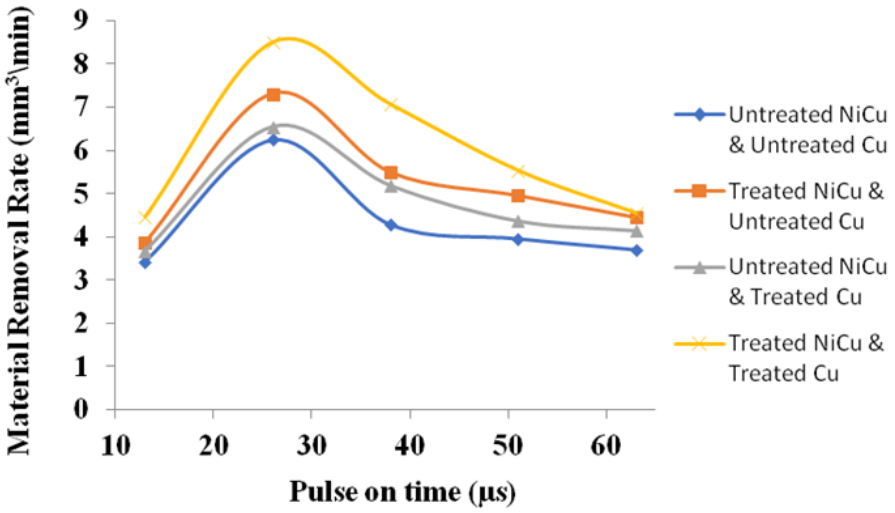

Figure 18. MRR versus pulse on time for NiCu alloy.

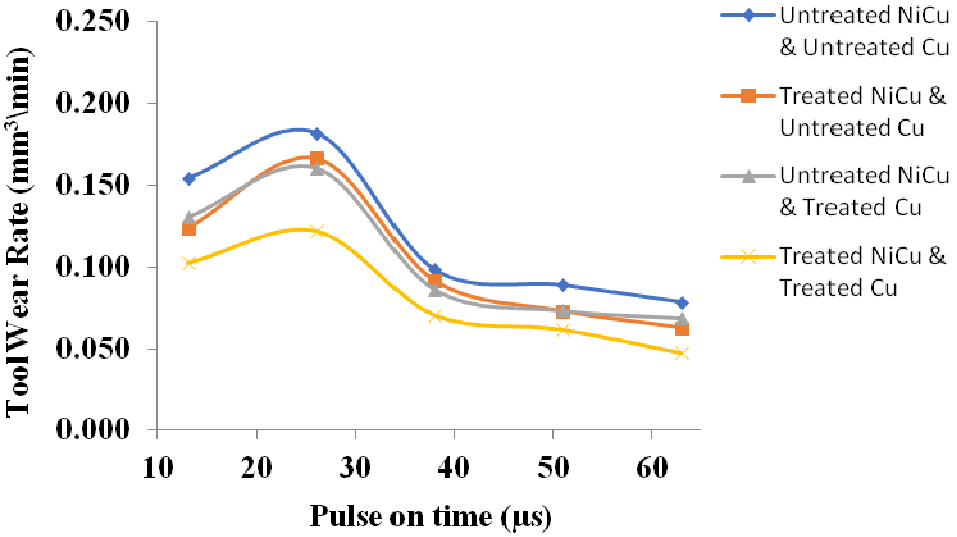

Figure 19. TWR versus pulse on time for NiCu alloy.

Based on the experimental results, a combination of four different pulse values with different BeCu-Cu configurations was evaluated, as shown in Table 11. Figure 20 shows the MRR against pulse on time for BeCu alloy and Cu combinations. In the presence of an increasing pulse on time, the MRR increased up to 26 µs. All four combinations of the pulse on time results resulted in decreasing MRR values with further increase in pulse on time. In this study, the maximum MRR value was obtained at a pulse on time of 26 µs (MRR = 6.086 mm^3/min). The TWR can be observed to be affected by the pulse on time for the BeCu alloy and Cu combinations in Figure 21. Up to a 26-µs pulse on time, the TWR increased; thereafter, it decreased. With the BeCu alloys and treated copper, the lowest TWR values were obtained.

Table 11. Results of exploratory experiments for BeCu alloy (pulse on time).

Sr. No.	Pulse on time (μs)	Untreated BeCu and Cu		Untreated BeCu and treated Cu		Treated BeCu and untreated Cu		Treated BeCu and treated Cu	
		MRR (mm^3/min)	TWR (mm^3/min)	MRR (mm^3/min)	TWR (mm^3/min)	MRR (mm^3/min)	TWR (mm^3/min)	MRR (mm^3/min)	TWR (mm^3/min)
1	13	1.232	0.0719	2.314	0.1427	2.018	0.0811	3.112	0.0469
2	26	4.127	0.1797	4.486	0.2224	5.295	0.3002	6.086	0.0853
3	38	3.189	0.1211	3.889	0.1509	4.538	0.1575	5.171	0.0532
4	51	2.902	0.1064	3.375	0.1489	3.624	0.1699	4.314	0.0505
5	63	2.632	0.0978	2.977	0.1056	3.465	0.1547	4.137	0.0450

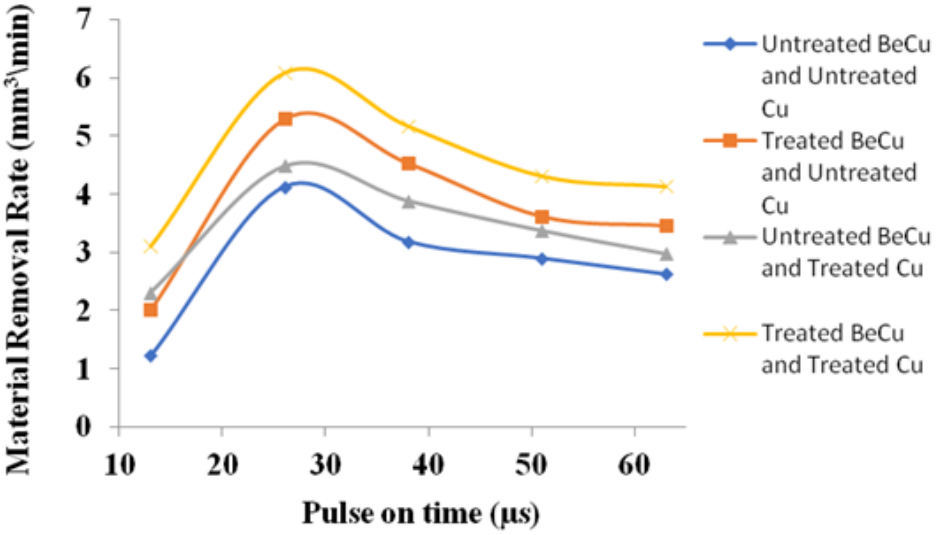

Figure 20. MRR versus pulse on time for BeCu alloy.

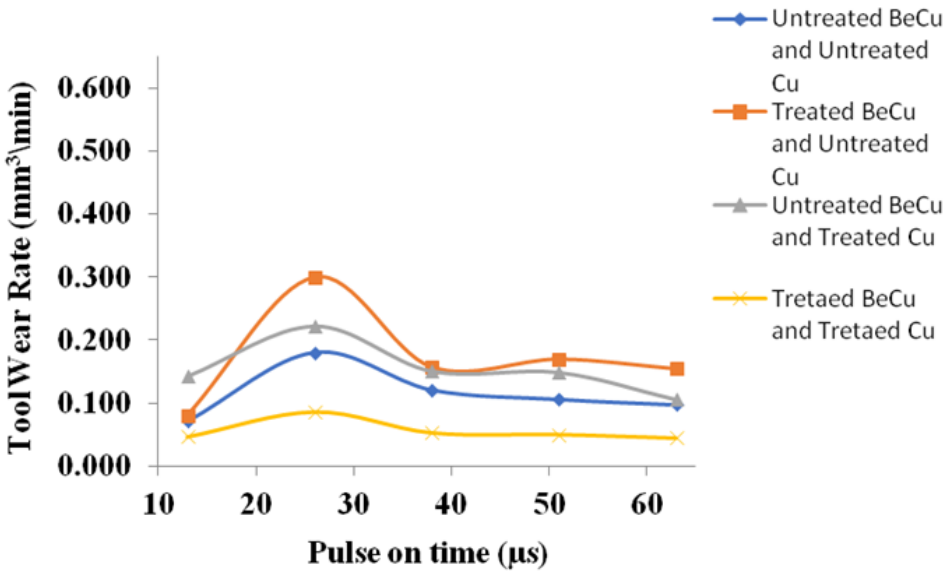

Figure 21. TWR versus pulse on time for BeCu alloy.

As a result of this carbon coating on the tool, the tool wears less and the TWR is lower. The MRR of the cryo-treated Cu electrode and NiTi alloy increased by 28.223%, and the TWR decreased by 19.845%; the MRR of the NiCu alloy and copper electrode increased by 38.894%; the MRR of the BeCu alloy and copper electrode increased by 73.589%, and the TWR decreased by 49.986%.

3.4. Impact of pulse off times on performance measures

We applied a step-by-step variation of the pulse off time. For the remaining parameters, the values were the gap voltage, gap current and pulse on time, i.e., 12 A, 55 V and 38 µs, respectively. In Table 12, the experimental values are given for different NiTi alloys and Cu combinations, as well as for different pulse off times.

Table 12. Results of exploratory experiments for NiTi alloy (pulse off time).

Sr. No.	Pulse off time (µs)	Untreated NiTi and Cu		Untreated NiTi and treated Cu		Treated NiTi and untreated Cu		Treated NiTi and treated Cu	
		MRR (mm^3/min)	TWR (mm^3/min)	MRR (mm^3/min)	TWR (mm^3/min)	MRR (mm^3/min)	TWR (mm^3/min)	MRR (mm^3/min)	TWR (mm^3/min)
1	5	4.773	0.214	4.711	0.046	5.517	0.093	5.271	0.027
2	6	4.290	0.096	4.072	0.032	5.413	0.084	4.618	0.025
3	7	4.019	0.088	3.930	0.027	4.413	0.082	4.296	0.024
4	8	4.008	0.082	3.734	0.021	4.134	0.060	3.821	0.019
5	9	3.879	0.078	3.171	0.017	3.776	0.046	3.171	0.011

Figure 22 shows the relationship between the MRR and pulse off time for different Cu and NiTi alloy combinations. A low pulse off time resulted in a low MRR. Increasing the pulse off time resulted in a decrease in the MRR. Using the untreated Cu and cyro-treated NiTi alloy, the maximum MRR was obtained. The MRR values for the treated Cu were second highest after the NiTi treated alloy. Figure 23 shows the TWR graph for various pulse off times and the four combinations. Increasing the pulse off time resulted in lower TWRs for all combinations. Similarly, the treated NiTi alloys and treated Cu alloys exhibited the lowest TWRs.

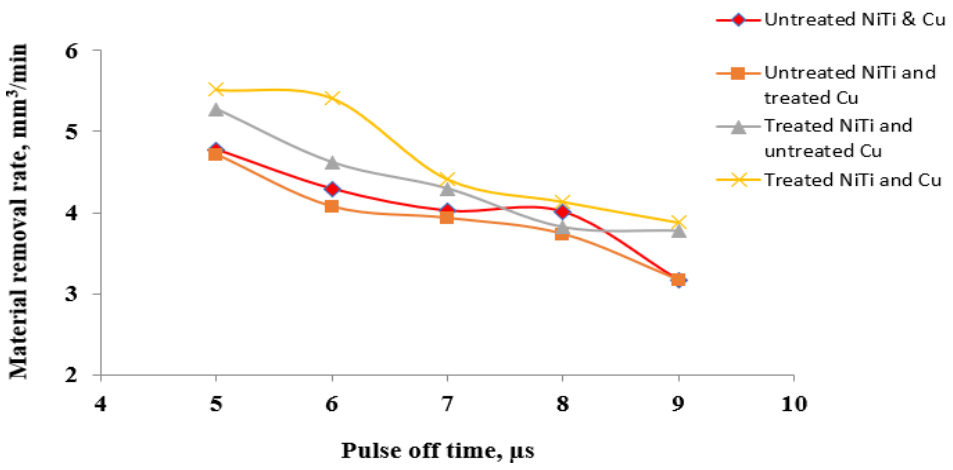

Figure 22. MRR versus pulse off time for NiTi alloy.

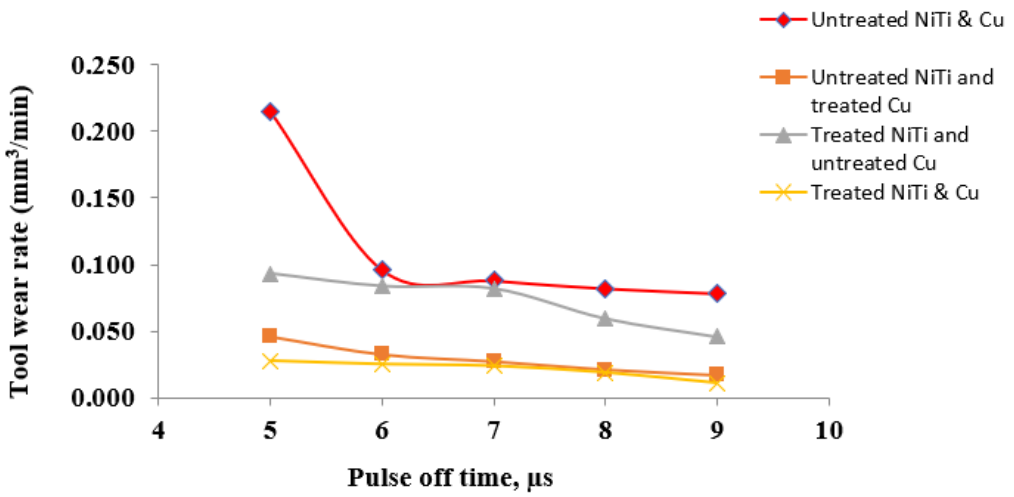

Figure 23. TWR versus pulse off time for NiTi alloy.

As shown in Table 13, comparing the results for the Cu and NiCu alloy for different off times was carried out. In Figure 24, one can see the pulse off time effects on the MRR of the Cu and NiCu alloy for the four different combinations. As a result of reducing the pulse off time, the MRR increased, and it decreased with increasing pulse off time. The MRR values for the treated NiCu alloy combined with the untreated Cu were the highest.

As seen in Figure 25, the TWR was affected by the pulse off time for the Cu and NiCu alloy combinations. There was a decrease in the TWR with an increase in pulse off time. Furthermore, the treated NiCu alloys and treated Cu exhibited the lowest TWRs.

Table 13. Results of exploratory experiments for NiCu alloy (pulse off time).

Sr. No.	Pulse off time (µs)	Untreated NiCu and Cu		Untreated NiCu and treated Cu		Treated NiCu and untreated Cu		Treated NiCuand treated Cu	
		MRR (mm^3/min)	TWR (mm^3/min)	MRR (mm^3/min)	TWR (mm^3/min)	MRR (mm^3/min)	TWR (mm^3/min)	MRR (mm^3/min)	TWR (mm^3/min)
1	5	4.917	0.0822	5.466	0.0679	6.551	0.0714	6.291	0.0669
2	6	4.253	0.0718	4.969	0.0642	6.323	0.0690	6.060	0.0609
3	7	4.210	0.0682	4.897	0.0593	6.130	0.0651	5.916	0.0562
4	8	4.038	0.0593	4.851	0.0474	5.775	0.0495	5.327	0.0372
5	9	3.777	0.0415	4.146	0.0322	4.826	0.0386	4.503	0.0302

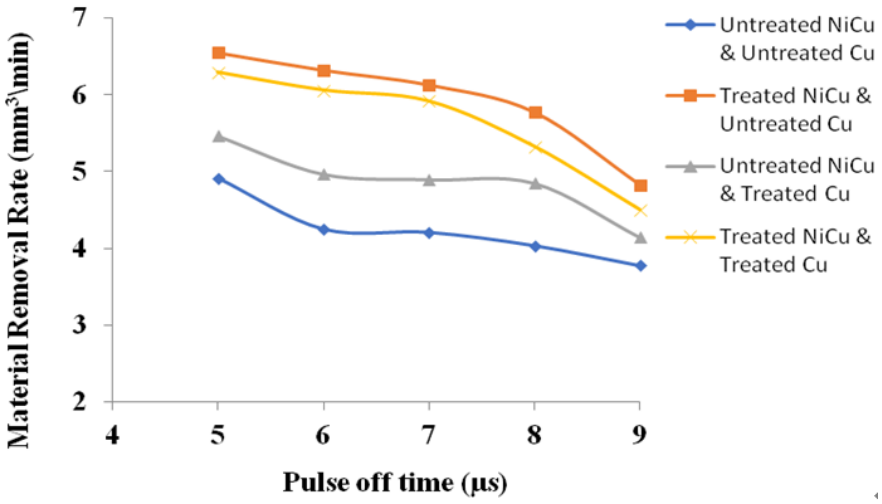

Figure 24. MRR versus pulse off time for NiCu alloy.

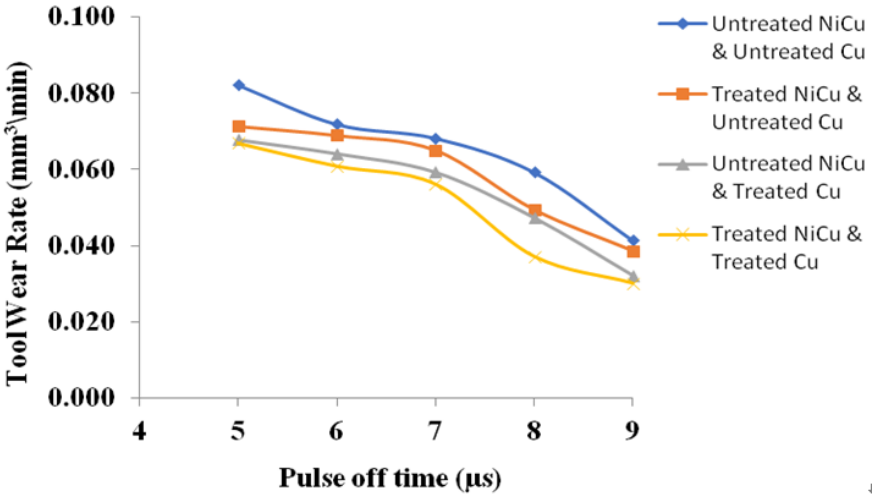

Figure 25. TWR versus pulse off time for NiCu alloy.

The experimental results are presented in Table 14 for the Cu and BeCu alloy combinations, and for varying pulse off times. Figure 26 shows the MRR plots for the BeCu alloy and Cu combinations. As the pulse off time increased for all combinations, the MRR decreased. The maximum MRR was achieved for the Cu and BeCu alloys.

In Figure 27, we show four combinations of the BeCu alloy and Cu as a function of pulse off time. With increasing pulse off time, a decrease in TWR can be observed. For both BeCu alloy and Cu treated, it is observed that TWR further decreases.

Table 14. Results of exploratory experiments for BeCu alloy (pulse off time).

Sr. No.	Pulse off time (μs)	Untreated BeCu and Cu		Untreated BeCu and treated Cu		Treated BeCu and untreated Cu		Treated BeCu and treated Cu	
		MRR (mm^3/min)	TWR (mm^3/min)	MRR (mm^3/min)	TWR (mm^3/min)	MRR (mm^3/min)	TWR (mm^3/min)	MRR (mm^3/min)	TWR (mm^3/min)
1	5	6.722	0.2735	6.192	0.1980	7.204	0.2504	7.302	0.1952
2	6	6.624	0.2769	6.300	0.1805	7.137	0.2331	7.196	0.1473
3	7	6.569	0.2496	5.629	0.1575	6.829	0.1970	6.922	0.1196
4	8	6.353	0.2237	4.987	0.1245	6.432	0.1679	6.645	0.0879
5	9	6.152	0.1881	4.827	0.0905	6.360	0.1491	6.474	0.0768

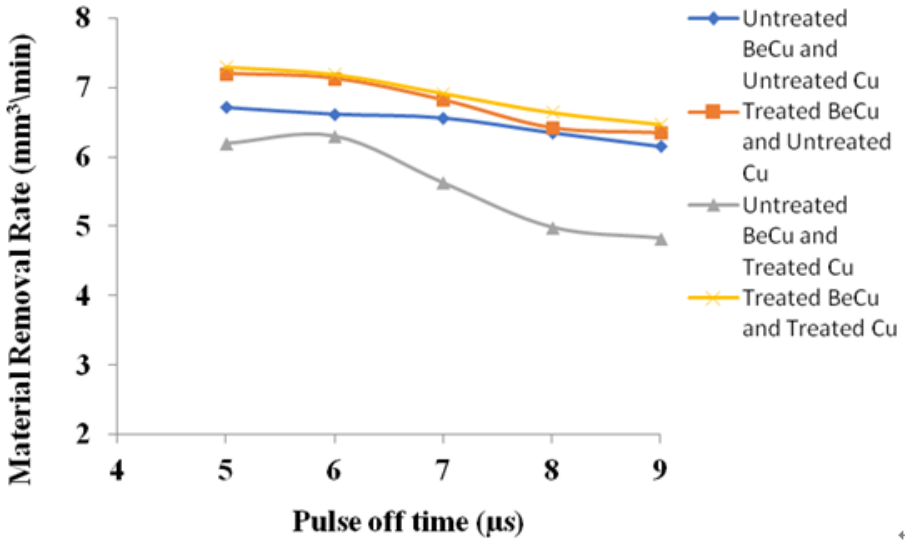

Figure 26. MRR versus pulse off time for BeCu alloy.

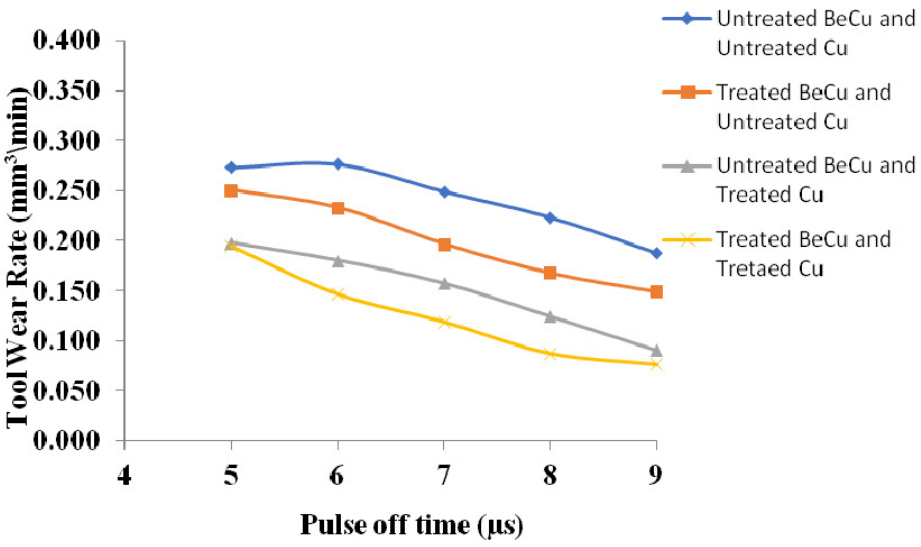

Figure 27. TWR versus pulse off time for BeCu alloy.

The cryogenic treatment of copper electrodes and NiTi alloys resulted in increased corrosion resistance; the MRR increased by 15.419%, while the TWR decreased by 79.649%; for the NiCu alloy and copper electrode, the MRR increased by 32.419%, while the TWR decreased by 23.183%; for the BeCu alloy and copper electrode, the MRR increased by 6.485%, while the TWR decreased by 49.479%.

4. Discussions

4.1. Effect of gap current

With an increase in gap current, the MRR increased regardless of whether or not the workpiece was cryogenically treated. Increasing the gap current increases the effective energy available in the machining area. A high gap current is reported to give a high current density. Furthermore, the expansion of the dielectric medium caused an increase in the impulsive force, allowing the working materials to melt and evaporate. Positive ions attack the workpiece surface more readily when the gap current increases. Consequently, the surface temperature of the workpiece rises, melting or evaporating the material. As a result, the crater size increases, leading to a higher MRR. With an increase in gap current, the MRR also increases, and cryogenic treatment can further enhance the MRR value. The spark energy, as well as the material of the tool, determines the rate of tool wear. Electrons move toward tool electrodes when an electric field is applied, resulting in a small-diameter plasma channel. By doing so, the tool surface is eroded.

4.2. Effect of gap voltage

When the gap voltage is lower, the inter-electrode spark gap will be smaller. If debris accumulates at the interface between the tool and the workpiece, it will cause damage. This leads to arcing, which results in the electrodes becoming corroded. The gap voltage affects the spark energy, which is well known. A low gap voltage reduces the spark energy and results in a lower MRR. This leads to a longer cycle time and longer exposure of the tool to machining conditions, which increases the wear rate. As a result, the tool wears more quickly. The electrode material becomes more electrically and thermally conductive after cryogenic treatment. There will be a smaller local temperature rise as a result. As a result of faster heat conduction to the bulk of the tool material, the tool wear is reduced for the same heat load.

4.3. Effect of pulse on time

The MRR is typically directly related to the discharge energy, which is determined by pulse duration. Increasing the pulse duration will lead to greater discharge energy. A greater number of positive ions from the plasma channel strikes the work surface. As a result of the bombardment of ions, the surface temperature of the workpiece increases. Hence, the rise in temperature melts the work material and increases the MRR. Increasing the pulse on time increases the plasma channel size; thus, the spark energy decreases. As a result, less heat and energy are transferred to the surface of the workpiece. Furthermore, the MRR decreases as the pulse time increases. A reduced discharge pressure inhibits the emergence of the molten metal difficult from the cutting zone. The TWR decreases with an

increase in pulse on time. Higher pulse on time values dissociate more carbon from the medium. Consequently, more carbon accumulates on the surface of the tool.

4.4. Effect of pulse off time

An EDM process utilizing a single discharge die sink was used in this study. Two sparks will occur after a time interval called the pulse off time, which means that two sparks will occur after some time has passed. It is during this time period that the dielectric fluid is deionized and the interface between the tool and the workpiece is reinsulated. The MRR and TWR are high at lower pulse off times due to the high spark energy at the interface between the workpiece and its tool. The TWR and MRR decrease with increasing pulse off time. Consequently, the plasma channel will decrease and the number of ions hitting the electrode surfaces will be reduced.

As a result of cryogenic treatment, the metal atoms are less likely to vibrate thermally, making them more susceptible to emitted electrons [4,6–13]. Electric bulk heating is reduced because electrons can easily be cold-emitted. Electrical resistance is reduced and electrical conductivity is improved. When crystals are cryo-treated, they become more homogeneous, the gaps are dissolved and the alloying elements are dislocated. As a result, the structure becomes more compact. Thus, the material becomes more electrically conductive [15–18]. Improved electrical conductivity causes increased thermal conductivity, according to the Wiedmann-Franz-Lorenz law [9].

The tool electrode considered in the present study was electrolytic copper, which has good thermal and electrical conductivity. These properties result in operational heat transfer to the workpiece, which then leads to the removal of a large amount of material from the workpiece. As a result, there is minimum erosion of the tool electrode material. It is very remarkable to note that, regardless of the type of workpiece (cryogenically treated or untreated) used, the MRR increased while machining with a cryogenically treated tool electrode. Hence, it can be concluded that the cryogenically treated tool electrode and workpiece each have their own role to play in improving the MRR, and their combined effect results in extra enhancement of the MRR.

5. Limitations

In this study, Nitinol (NiTi), Monel (NiCu) and beryllium copper (BeCu) workpieces and copper as electrode materials were studied. The experiment investigated the effect of cryogenic treatment, as well as the parameters of an EDM machine, namely, the gap current, pulse off time and pulse on time, on the MRR and TWR.

6. Conclusions

EDM process parameters, such as the gap current, gap voltage, workpiece electrical conductivity and pulse on-off time, were investigated during the machining of advanced materials. Based on the results of this study, the cryogenically treated workpieces and electrodes had significantly better electrical conductivity. Regarding the removal rate and reducing tool wear, the cryogenic treatment of workpieces and tool materials was observed to improve both. The MRR and TWR for the NiTi alloys increased after cryogenic treatment based on the gap current selection from 8 A to 16 A. After cryogenic treatment, the MRR increased by 16.190% and the TWR decreased by 23.244% when the

gap voltage was further increased. As the pulse on time was increased from 13 to 63 μs, the MRR increased by 28.223% and the TWR decreased by 19.845%. The MRR and TWR decreased by 79.649% and 15.419%, respectively, after cryogenic treatment. Increasing the pulse off time increased the MRR by 32.419% and TWR by 23.183% after cryogenic treatment. During cryogenic treatment of the BeCu alloy, the MRR increased by 87.548% and the TWR decreased by 42.587% due to gap currents. The MRR and TWR, after cryogenic treatment, were increased by 34.155% and 44.272%, respectively, due to the gap voltage. The overall MRR and TWR, after cryogenic treatment, increased by 73.589% and 49.986%, respectively. After cryogenic treatment, the MRR increased by 6.485% and the TWR decreased by 49.479% with increasing pulse off time.

6.1. Future work

In a later study, will investigate the effect of the cryogenic treatment of workpieces and tools, along with the EDM machine parameters, on surface morphology, namely, the SR, white layer thickness, surface crack density and residual stresses of the EDM machined workpiece.

Acknowledgments

We acknowledge the Symbiosis Institute of Technology, Symbiosis International (Deemed University), Pune, Maharashtra, India for support for the open-access publication fees.

Conflict of interest

The authors declare that they have no conflict of interest.

References

1. Sharma A, Mohanty CP, Pardasani K (2018) Finite element analysis of cryogenically treated EDM. *Mater Today Proc* 5: 19367–19373. https://doi.org/10.1016/j.matpr.2018.06.296
2. Tharian BK, Dhanish PB, Manu R (2021) Enhancement of material removal rate in Electric Discharge Machining of Inconel 718 using cryo-treated graphite electrodes. *Mater Today Proc* 47: 5172–5176. https://doi.org/10.1016/j.matpr.2021.05.506
3. Singh J, Singh G, Pandey PM (2021) Electric discharge machining using rapid manufactured complex shape copper electrode with cryogenic cooling channel. *P I Mech Eng B-J Eng* 235: 173–185. https://doi.org/10.1177/0954405420949102
4. Prakash D, Tariq M, Davis R, et al. (2021) Influence of cryogenic treatment on the performance of micro-EDM tool electrode in machining of magnesium alloy AZ31B. *Mater Today Proc* 39: 1198–1201. https://doi.org/10.1016/j.matpr.2020.03.589
5. Shastri RK, Mohanty CP, Dash S, et al. (2022) Reviewing performance measures of the die-sinking electrical discharge machining process: Challenges and future scopes. *Nanomaterials* 12: 384. https://doi.org/10.3390/nano12030384
6. Abdulkareem S, Khan AA, Konneh M (2009) Reducing electrode wear ratio using cryogenic cooling during electrical discharge machining. *Int J Adv Manuf Tech* 45: 1146–1151. https://doi.org/10.1007/s00170-009-2060-5

7. Gill SS, Singh J (2010) Effect of deep cryogenic treatment on machinability of titanium alloy (Ti-6246) in electric discharge drilling. *Mater Manuf Process* 25: 378–385. https://doi.org/10.1080/10426910903179914
8. Srivastava V, Pandey PM (2012) Performance evaluation of electrical discharge machining process using cryogenically cooled electrode. *Mater Manuf Process* 27: 683–688. https://doi.org/10.1080/10426914.2011.602790
9. Yildiz Y, Sundaram M M, Rajurkar K P, Nalbant M (2011) The effects of cold and cryogenic treatments on the machinability of beryllium-copper alloy in electro discharge machining. *Proceedings of 44th CIRP Conference on Manufacturing Systems*, Madison, USA, 1–6.
10. Singh R, Singh B (2011) Comparison of cryo-treatment effect on machining characteristics of titanium in electric discharge machining. *Int J Automo Mech E* 3: 239–248. https://doi.org/10.15282/ijame.3.2011.1.0020
11. Gill AS, Kumar S (2012) Wear reduction of aluminium electrode by cryogenic treatment in electric discharge machining. *Int J Surf Eng Mater Technol* 2: 19–23.
12. Nadig DS, Ramakrishnan V, Sampathkumaran P, et al. (2012) Effect of cryogenic treatment on thermal conductivity properties of copper. *AIP Conf Proc* 1435: 133–139. https://doi.org/10.1063/1.4712089
13. Srivastava V, Pandey PM (2012) Effect of process parameters on the performance of EDM process with ultrasonic assisted cryogenically cooled electrode. *J Manuf Process* 14: 393–402. https://doi.org/10.1016/j.jmapro.2012.05.001
14. Liqing L, Yingjie S (2013) Study of dry EDM with oxygen-mixed and cryogenic cooling approaches. *Procedia CIRP* 6: 344–350. https://doi.org/10.1016/j.procir.2013.03.055
15. Jafferson JM, Hariharan P (2013) Machining performance of cryogenically treated electrodes in microelectric discharge machining: A comparative experimental study. *Mater Manuf Process* 28: 397–402. https://doi.org/10.1080/10426914.2013.763955
16. Mathai VJ, Vaghela RV, Dave HK, et al. (2013) Study of the effect of cryogenic treatment of tool electrodes during electro discharge machining. *International conference on Precision, Meso, Micro and Nano Engineering*, Kerala, India, 679–684.
17. Ram NR, Rao KV, Kanth CL, et al. (2014) Parametric analysis on the effect of cryogenic treatment on the work piece material of EDM Process. *Int J Eng Res Technol* 3: 1087–1094.
18. Kumar SV, Kumar MP (2014) Optimization of cryogenic cooled EDM process parameters using grey relational analysis. *J Mech Sci Technol* 28: 3777–3784. https://doi.org/10.1007/s12206-014-0840-9

AIMS Press